Design and Characterization of an Improved Protein Tyrosine Phosphatase Substrate-Trapping Mutant†

Laiping Xie, Yan-Ling Zhang,‡ and Zhong-Yin Zhang*

Department of Molecular Pharmacology, Albert Einstein College of Medicine, 1300 Morris Park Avenue, Bronx, New York 10461

Received October 31, 2001; Revised Manuscript Received January 14, 2002

ABSTRACT: Although members of the protein tyrosine phosphatase (PTPase) family share a common mechanism of action (hydrolysis of phosphotyrosine), the cellular processes in which they are involved can be both highly specialized and fundamentally important. Identification of cellular PTPase substrates will help elucidate the biological functions of individual PTPases. Two types of substrate-trapping mutants are being used to isolate PTPase substrates. In the first, the active site Cys residue is replaced by a Ser (e.g., PTP1B/C215S) while in the second, the general acid Asp residue is substituted by an Ala (e.g., PTP1B/D181A). Unfortunately, only a limited number of PTPase substrates have been identified with these two mutants, which are usually relatively abundant cellular proteins. Based on mechanistic considerations, we seek to create novel PTPase mutants with improved substrate-trapping properties. Kinetic and thermodynamic characterization of the newly designed PTP1B mutants indicates that PTP1B/D181A/Q262A displays lower catalytic activity than that of D181A. In addition, D181A/Q262A also possesses 6- and 28-fold higher substrate-binding affinity than those of D181A and C215S, respectively. In vivo substrate-trapping experiments indicate that D181A/Q262A exhibits much higher affinity than both D181A and C215S for a bona fide PTP1B substrate, the epidermal growth factor receptor. Moreover, D181A/Q262A can also identify novel, less abundant substrates, that are missed by D181A. Thus, this newly developed and improved substrate-trapping mutant can serve as a powerful affinity reagent to isolate and purify both high- and low-abundant protein substrates. Given that both Asp181 and Gln262 are invariant among the PTPase family, it is predicted that this improved substrate-trapping mutant would be applicable to all members of PTPases for substrate identification.

Sequencing of the human and other genomes has radically changed the ways in which we identify and characterize genes. Typically, database searches based on structural similarities can assign a gene product to an established protein family. Although members of protein families often share a common mechanism of action, the cellular processes in which they are involved can be both highly specialized and fundamentally important. Protein tyrosine phosphatases (PTPases),[1] which have conserved catalytic domains but are involved in controlling a broad constellation of cellular processes (*1*−*3*), provide a striking example of conserved structures associated with functional diversity. The hallmark that defines the PTPase superfamily is the active site amino acid sequence (H/V)**C**(X)$_5$**R**(S/T), also referred to as the PTPase signature motif, within the catalytic domain. To date, analysis of the nearly completed human genome has revealed 112 predicted human PTPases (*4*). Therefore, it is relatively easy to attribute a general role to a PTPase gene product based on structural homologies. However, determination of the exact physiological function of a PTPase requires a tedious and protracted effort. Identification of the cellular substrates of individual PTPases will help elucidate the biological functions of individual PTPases. A major challenge, though, is the development of technologies for rapid substrate identification that can be applied to the entire PTPase family.

Detailed mechanistic studies have shown that PTPases utilize a common mechanism for phosphomonoester hydrolysis (Figure 1) (*5*). In particular, the PTPases employ the active site cysteine (Cys215 in PTP1B) as the attacking nucleophile, thereby forming a thiophosphoryl enzyme intermediate (E−P) (*6*, *7*). The E−P formation is assisted by a conserved aspartic acid (Asp181 in PTP1B), functioning as a general acid, to neutralize the build-up of a negative charge on the leaving group (*8*, *9*). For the hydrolysis of E−P, Asp181, previously functioning as a general acid in E−P formation, acts as a general base, abstracting a proton from the attacking water (*10*, *11*). This enhances the rate of

† This work was supported in part by National Institutes of Health Grant GM55242. L.X. is supported by a Fellowship from AstraZeneca. Z.-Y.Z. is an Irma T. Hirschl Career Scientist.

* To whom correspondence should be addressed. Phone: 718-430-4288. FAX: 718-430-8922. E-mail: zyzhang@aecom.yu.edu.

‡ Current address: Genetics Institute, 200 Cambridge Park Dr., Cambridge, MA 02140.

[1] Abbreviations: PTPase, protein tyrosine phosphatase; PTP1B, protein tyrosine phosphatase 1B; EGF, epidermal growth factor; pY or pTyr, phosphotyrosine; F_2Pmp, phosphonodifluoromethyl phenylalanine; *p*NPP, *p*-nitrophenyl phosphate; EDTA, ethylenediaminetetraacetic acid; ITC, isothermal titration microcalorimetry; HRP, horseradish peroxidase; HA, hemagglutinin; SDS−PAGE, sodium dodecyl sulfate−polyacrylamide gel electrophoresis.

10.1021/bi015904r CCC: $22.00
Published on Web 02/27/2002

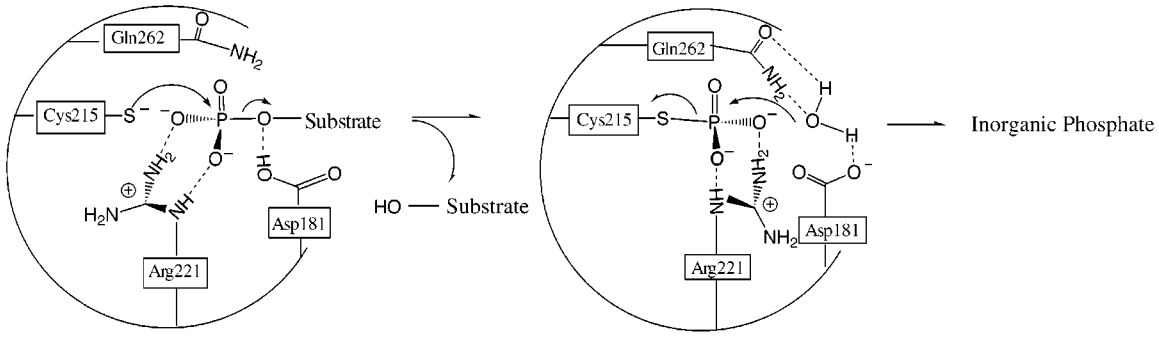

FIGURE 1: A chemical mechanism for the PTP1B-catalyzed dephosphorylation reaction.

E−P hydrolysis, thereby regenerating the active enzyme. The rate of E−P hydrolysis is also increased by a conserved active site glutamine (Gln262 in PTP1B), which positions the nucleophilic water for E−P hydrolysis (*12*−*14*). The PTPases further accelerate the formation and hydrolysis of E−P by preferentially binding the pentacoordinated transition states with the guanidinium side chain of the active site arginine residue (Arg221 in PTP1B) (*15*, *16*).

Because of the transient nature of the enzyme·substrate complex, it has been difficult to isolate substrates with wild-type PTPases. Based on insights from mechanistic studies, two types of "substrate-trapping" mutant PTPases have been developed. In the first, the active site Cys residue is replaced by a Ser (*17*−*19*) while in the second, the general acid Asp residue is substituted by an Ala (*20*, *21*). These mutants retain the ability to bind substrates; however, because they are either unable to carry out substrate dephosphorylation (the Cys to Ser mutant) or severely impaired in carrying out substrate dephosphorylation (the Asp to Ala mutant), capture of the PTPase·substrate complex becomes possible.

These substrate-trapping mutants have been used as affinity reagents to isolate and identify physiological substrates for various PTPases. Nevertheless, to date, only a limited number of PTPase substrates have been identified by the substrate-trapping approach, and these have been mostly abundant proteins. For example, the adapter protein $p130^{Cas}$ has been found to be the target of several PTPases, including PTP1B (*22*), PTP-PEST (*20*), the *Yersinia* PTPase (*23*), PTPα (*24*), LAR (*25*), and SAP (*26*). The fact that only a few proteins have been identified as PTPase substrates is surprising, given the large number of protein tyrosine kinases and pTyr-containing proteins in the cell. One possible explanation may be that the affinity of the available trapping mutants is not sufficiently high, such that only heavily populated phosphoproteins can be isolated. Therefore, there exists a need to create an improved PTPase substrate-trapping mutant, with a higher affinity, that will enable the identification of less abundant substrates.

We describe here the design and characterization of an improved PTP1B substrate-trapping mutant (D181A/Q262A) that displays 6- and 28-fold higher affinity than the existing D181A and C215S mutants, respectively. Because both Asp181 and Gln262 are invariant among PTPases (*27*), this double mutant should be applicable to all members of the PTPase family for substrate identification. Identification and characterization of specific PTPase/substrate interactions will associate functions with individual PTPases as well as implicate specific PTPases to specific signaling pathways.

MATERIALS AND METHODS

Materials. *p*-Nitrophenyl phosphate (*p*NPP) was purchased from Fluka Co. Other chemicals were from Fisher Co. Solutions were prepared using deionized and distilled water. The preparation of the nonhydrolyzable pTyr mimetic phosphonodifluoromethyl phenylalanine (F_2Pmp)-containing peptide Ac-Asp-Ala-Asp-Glu-F_2Pmp-Leu-NH_2 was described (*28*). Recombinant human epidermal growth factor (EGF) was purchased from Upstate Biotechnology (Lake Placid, NY). Anti-hemagglutinin (HA) epitope mouse monoclonal antibody IgG−horseradish peroxidase (HRP) conjugate, anti-phosphotyrosine antibody PY20 and PY99 horseradish peroxidase conjugated, anti-HA conjugated agarose for immunoprecipitation, rabbit anti-EGF receptor polyclonal antibody, and goat anti-rabbit IgG−HRP were all from Santa Cruz Biotechnology.

Protein Expression and Purification. The catalytic domain of PTP1B (residues 1−321) was used for in vitro study. PTP1B mutants C215S, D181A, and Q262A were described previously (*9*, *14*, *29*). PTP1B double mutants D181A/C215S and C215S/Q262A were generated by PCR reactions according to the standard procedure of the Quick-Change site-directed mutagenesis kit (Stratagene) using pT7-7/PTP1B/C215S as a template. PTP1B double mutants D181A/C215E and D181A/Q262A were generated by similar PCR procedures using pT7-7/PTP1B/D181A as a template. The recombinant wild-type and mutant PTP1Bs were expressed in *E. coli* and purified to homogeneity as described (*29*, *30*). Protein concentration was determined from absorbance measurement at 280 nm using an absorbance coefficient 1.24 for 1 mg/mL PTP1B.

Determination of Kinetic Constants Using pNPP as a Substrate. The PTPase activity was assayed at 25 °C and pH 7.0 in a reaction mixture (0.2 mL) containing *p*NPP concentrations ranging from $0.2K_m$ to $5K_m$. The following buffered solution was used for activity measurements: pH 7.0, 50 mM 3,3-dimethylglutarate, 1 mM EDTA, ionic strength = 0.15 M adjusted by addition of NaCl. Initial rate measurements for the enzyme-catalyzed hydrolysis of *p*NPP were conducted as previously described (*14*). Michaelis−Menten kinetic parameters were determined from a direct fit of the data to the Michaelis−Menten equation using the nonlinear regression program KINETASYST (Intellikinetics, State College, PA).

Determination of Kinetic Constants Using pTyr-Containing Peptides as Substrates. All assays were performed at 25 °C in pH 7, 50 mM 3,3-dimethylglutarate, 1 mM EDTA, ionic strength of 0.15 M, buffer. A continuous spectrophotometric

assay described previously was employed to determine k_{cat} and K_m for the pTyr-containing peptides (*31*). The dephosphorylation reaction can be monitored by either an increase in absorbance at 282 nm or an increase in fluorescence at 305 nm. Fluorometric and absorbance determinations were performed on a Perkin-Elmer LS50B fluorometer and a Perkin-Elmer Lambda 14 spectrophotometer, respectively. The instruments were equipped with a water-jacketed cell holder, permitting maintenance of the reaction mixture at the desired temperature (25 °C).

Isothermal Titration Calorimetry. All isothermal titration calorimetry experiments were performed using a MCS Isothermal Titration Calorimetry System from Microcal Inc., Northampton, MA. Experiments at pH 7.0 were conducted at 25 °C, in 50 mM 3,3-dimethylglutarate buffer, containing 1 mM DTT. The ionic strength of the buffer was adjusted to 0.15 M by addition of NaCl. Protein concentration in the calorimeter cell was 27−85 μM, while the ligand concentration in the syringe was 0.37−1 mM. The PTP1B samples used in the isothermal titration calorimetry experiments were dialyzed completely against buffer. High concentration stock solutions were prepared for ligands with distilled water and adjusted to pH 7.0. Stock was diluted at least 26-fold with 50 mM 3,3-dimethylglutarate buffer before titration. Protein dilution during titration was determined by titration of buffer into the protein solution. The heat of protein dilution was found to be negligible. The heat of ligand dilution was corrected by subtracting the average heat of injection after saturation. The binding data were analyzed using Origin software (*32*). Binding constants K and enthalpy changes ΔH were used to calculate free energy change ΔG and entropy change ΔS according to eq 1:

$$-RT \ln K = \Delta G = \Delta H - T\Delta S \quad (1)$$

where R is the gas constant and T is the absolute temperature.

Mammalian Expression Plasmids. The HA-tagged full-length human wild-type PTP1B in pJ3H expression vector was a gift from Dr. Chernoff (*33*). The HA-tagged PTP1B mutants C215S, D181A, D181A/C215S, and D181A/Q262A were generated by PCR reactions according to the standard procedure of the Quick-Change site-directed mutagenesis kit (Stratagene) using pJ3H-HA-PTP1B as a template. All mutations were verified by DNA sequencing.

Cell Culture and Transient Transfection. Monkey kidney COS1 cells (ATCC, CRL-1650) were maintained in Dulbecco's modified Eagle's minimum essential medium (DMEM) supplemented with 10% fetal bovine serum (Life Technologies, Inc.), penicillin (50 units/mL), streptomycin (50 μg/mL), and L-glutamine (2 mM) under a humidified atmosphere containing 5% CO_2. In transient transfection experiments, COS1 cells were inoculated at a density of 2×10^5 cells/60 mm dish, and grown overnight in DMEM containing 10% fetal bovine serum. Transfection was performed using LipoTAXI according to the manufacturer's recommendations (Stratagene, Cedar Creek, TX). Each transfection assay included 4 μg of purified DNA mixed with LipoTAXI in a 1:5 DNA:lipid ratio per 60 mm dish of cells. Following transfection, the cells were exchanged to normal culture medium and maintained for 44−48 h at 37 °C and 5% CO_2. The efficiency of transfection, as assessed by 5-bromo-4-chloro-3-indolyl β-D-galactoside (X-Gal) staining of pCMV-β-gal (β-Gal staining kit, Invitrogen) transfected COS cells, was 25%.

Cell Lysis, Immunoprecipitation, and Western Blotting. The transfected cells (treated with or without EGF) were lysed with "lysis buffer" containing 50 mM Tris-HCl, pH 7.5, 5 mM EDTA, 150 mM NaCl, 10 mM sodium phosphate, 10 mM sodium fluoride, 5 mM iodoacetic acid, 1 mM benzamidine, 1% Triton X-100, 10 μg/mL leupeptin, and 5 μg/mL aprotinin. Lysate protein concentration was estimated using Bio-Rad protein assay reagent (Bio-Rad, Hercules, CA). For immunoprecipitation, 1 mg of cell lysate was immunoprecipitated with 30 μL of agarose-conjugated anti-hemagglutinin antibody at 4 °C overnight. Immunocomplexes were washed 4 times with the cell lysis buffer and boiled for 5 min in SDS−PAGE sample buffer. Proteins in the cell lysate were separated by 8% SDS−PAGE under reducing conditions according to the method of Laemmli (*34*) followed by blotting onto nitrocellulose membranes (Protran, Schleicher & Schuell). The membranes were blocked with 5% nonfat dry milk in Tris-buffered saline−Tween (TBST) buffer (20 mM Tris-HCl, 150 mM NaCl, 0.1% Tween-20, pH 7.6) for 1 h at 25 °C. Thereafter, blots were incubated overnight with primary antibodies diluted in TBST containing 5% nonfat dry milk at 4 °C. The blots were then rinsed with TBST (3 times) for 5 min at 25 °C and incubated with the appropriate secondary antibody diluted in TBST containing 5% nonfat dry milk for 1 h at 25 °C. The blots were rinsed 3 more times with TBST for 5 min before detection by enhanced chemiluminescence (ECL) (Cell Signaling Technology). For reprobing, blots were stripped by incubating in 62.5 mM Tris-HCl, 2% SDS, 100 mM 2-mercaptoethanol (pH 6.7) for 30 min at 50 °C. Stripped blots were then rinsed extensively with TBST, and reprobed as described above.

RESULTS AND DISCUSSION

PTPases play a central role in controlling many diverse signal transduction pathways in all cells. Thus, although PTPases share a common catalytic mechanism (hydrolysis of phosphoamino acids), they have distinct (and often unique) biological functions in vivo. Genetics and biochemical studies indicate that PTPases are involved in a number of disease processes (*3*). However, despite the detailed understanding of PTPase catalysis, the molecular basis for the diverse biological functions of PTPases is poorly understood. In part, this lack of understanding is a result of the paucity of information concerning the physiological substrates of most PTPases. Therefore, identification of physiological substrates for individual PTPases remains one of the central goals in the field. An effective strategy to identify and characterize in vivo PTPase substrates is to employ high-affinity PTPase substrate-trapping mutants.

Currently, two types of substrate-trapping mutants are being used to identify PTPase substrates. The first involves the replacement of the active site Cys residue by a Ser, which leads to a complete loss of phosphatase activity (*17*−*19*, *35*). In the second, the general acid Asp residue is substituted by an Ala (*20*, *21*), which results in a decrease in k_{cat} of several orders of magnitude (*8*, *21*). So far, only relatively abundant cellular proteins have been identified with these two mutants. It is possible that the affinity of the existing trapping mutants for substrates is not high enough to enable the capture of

less abundant proteins. The goal of this study is to create a mutant PTPase with enhanced substrate trapping properties, for use in PTPase substrate identification.

Our strategy to achieve this goal is to exploit the common mechanism of PTPase catalysis to create substrate-trapping mutants that can be applied to all PTPase members. We decided to focus on invariant residues that are important for PTPase catalysis. There are two ways to improve a substrate-trapping mutant. One is to lower the dissociation constant (K_d) between the enzyme and the substrate, and the other is to further slow substrate turnover (k_{cat}). Since PTP1B/D181A displays higher affinity for substrates than C215S both in vitro and in vivo (*21*, *28*), we seek to improve its potency by introducing into it a second site mutation. Because the general acid deficient mutant D181A still contains residual phosphatase activity, we considered mutating additional invariant residues to further reduce its activity and to possibly further increase its binding affinity. The criteria for selecting the second site mutations are the following: (1) mutation of the second residue must lead to either further decrease in activity or increase in affinity, and (2) mutation of the second residue must not alter substrate specificity. Thus, the residues chosen ideally should be located in or near the active site pocket (i.e., pTyr binding site) and perform universal catalytic functions.

The active site Cys215 is an obvious choice because of its essential role in catalysis. Thus, substitutions of Cys215 in D181A should render the double mutant inactive. However, because the side chain of the active site Cys exists as a thiolate anion at physiological pH (*36*), the Cys to Ser mutation is not a simple substitution of OH for SH, but rather a replacement of the negatively charged thiolate anion with a neutral hydroxyl group. Indeed, we have observed that the Cys to Ser mutation causes significant structural/dynamic perturbations in the active site (*28*, *35*, *37*, *38*). Thus, in addition to D181A/C215S, we also prepared D181A/C215E in order to mimic the thiolate anion in the active site.

The next residue we chose was Gln262, which is invariant among all PTPases (Figure 2). The crystal structure of PTP1B/C215S bound with Ac-DADEpYL-NH_2 showed that the side chain of Gln262 is close to the phenyl ring of pTyr and may define a portion of the rim for the pTyr binding pocket (*39*). Previous kinetic studies revealed that the k_{cat}/K_m and k_{cat} for the PTP1B/Q262A-catalyzed hydrolysis of the epidermal growth factor receptor peptide DADEpYLIPQQG (EGFR$^{988-998}$) and phosphorylated lysozyme were reduced by 10- and 100-fold, respectively (*14*, *21*). This suggests that Gln262 may play a role in both E−P formation and the E−P hydrolysis step. Work on the structural equivalent Gln446 in the *Yersinia* PTPase (*12*) and Gln262 in PTP1B (*13*, *14*, and Gordon et al., unpublished results) also suggest that the invariant Gln262 residue is important for the optimal positioning of the nucleophilic water molecule for efficient E−P hydrolysis (Figure 1). To determine whether mutation of Gln262 would improve the existing substrate-trapping mutants, we prepared C215S/Q262A and D181A/Q262A.

Kinetic Characterization. All recombinant PTP1B proteins were expressed in *Escherichia coli* and purified to near-homogeneity as judged by SDS−polyacrylamide gel electrophoresis using procedures described previously (*29*, *30*) (data not shown). The kinetic parameters for the wild-type and mutant PTP1B-catalyzed hydrolysis of *p*NPP are summarized in Table 1. Table 2 lists the steady-state kinetic parameters for the wild-type and mutant PTP1Bs using the EGFR$^{988-998}$ peptide DADEpYLIPQQG as a substrate. As expected, no measurable activities were observed for C215S, D181A/C215S, C215S/Q262A, and D181A/C215E. For the D181A mutant, the k_{cat} was 320-fold lower than that of the wild-type enzyme while the K_m value was 30-fold lower with *p*NPP as a substrate (Table 1). With the EGFR$^{988-998}$ peptide as a substrate, the k_{cat} value for D181A was 920-fold lower

```
                    262
PTP1B   VLLEMRKFRM GLIQTADQLR
TcPTP   VLLNMRKYRM GLIQTPDQLR
HDPTP   LVRRMRQQRK HMLQEKLHLR
SHPTP1  TIQMVRAQRS GMVQTEAQYK
SHPTP2  TIQMVRSQRS GMVQTFAQYR
PTP-PEST LIQEMRTQRH SAVQTKEQYE
PTP-MEG1 IVRTMRDQRA MMIQTPSQYR
PTP-MEG2 TVSRMRTQRA FSIQTPEQYY
PTPH1   IVRKMRDQRA MMVQTSSQYK
GLEPP1  LVSEMRSYRM SMVQTEEQYI
BDP1    VVLKMRKQRP AAVQTEEQYR
HePTP   IVCQLRLDRG GMIQTDEQYQ
STEP    TTCQLRQDRG GMIQHCEQYQ
PCPTP1  IVQCLRMDRG GMVQTSEQYE
PTPD1   VLDMLRQQRM MLVQTLCQYT
PTPD2   MLRLLREQRM FMIQTIAQYK
PTPBAS  LVRCMRLQRH GMVQTEDQYI
CD45    YVVKLRRQRC LMVQVEAQYI
LAR     HVTCMRSQRN YMVQTEDQYV
PTPα    FVSRIRAQRC QMVQTDMQYV
PTPβ    AVHDLRLHRV HMVQTECQYV
PTPγ    FLKHIRTQRN YLVQTEEQYI
PTPδ    HVTLMRAQRN YMVQTEDQYI
PTPε    FVSRIRNQRP QMVQTDMQYT
PTPζ    FLKHIRSQRN YLVQTEEQYV
PTPσ    HVTLMRSQRN YMVQTEDQYS
PTPρ    CVRELRAQRV NLVQTEEQYV
PTPκ    CVKALRSRRI NMVQTEEQYI
PTPμ    CVRELRSRRV NMVQTEEQYV
PTPλ    CVKTLCSRRV NMIQTEEQYI
DEP-1   IVYDLRMHRP LMVQTEDQYV
SAP-1   FVRKMRESRP LMVQTEAQYV

yPTP1   IVLQLRSQRM KMVQTKDQFL
yPTP2   IVNELRKQRI SMVQNLTQYI

YOP51   MVSQMRVQRNGIMVQKDEQLD
```

FIGURE 2: Amino acid sequence alignment of 32 human PTPases, 2 yeast PTPases, and the *Yersinia* PTPase YOP51 surrounding Gln262 in PTP1B. Conserved residues are shown in boldface type.

Table 1: Kinetic Parameters for the Wild-Type and Mutant PTP1B-Catalyzed Hydrolysis of *p*NPP

PTP1B	K_m (μM)	k_{cat} (s^{-1})	k_{cat}/K_m ($M^{-1}\,s^{-1}$)
wild type[a]	2400 ± 200	9.8 ± 0.5	$(4.1 \pm 0.4) \times 10^3$
D181A[a]	80 ± 30	$(3.1 \pm 0.3) \times 10^{-2}$	$(3.9 \pm 1.5) \times 10^2$
Q262A[b]	58 ± 6	0.21 ± 0.01	$(3.6 \pm 0.3) \times 10^3$
D181A/Q262A[a]	2.4 ± 0.5	$(2.8 \pm 0.1) \times 10^{-3}$	$(1.2 \pm 0.2) \times 10^3$
C215S[c]			
D181A/C215S[c]			
C215S/Q262A[c]			
C215S/Q262A[c]			

[a] Measured at 25 °C and pH 7.0. [b] Measured at 30 °C and pH 7.0 (*14*). [c] No measurable activities were observed for C215S, C215S/D181A, C215S/Q262A, and D181A/C215E.

Table 2: Kinetic Parameters for the Wild-Type and Mutant PTP1B-Catalyzed Hydrolysis of $EGFR^{988-998}$, DADEpYLIPQQG

PTP1B	K_m (μM)	k_{cat} (s^{-1})	k_{cat}/K_m (M^{-1} s^{-1})
wild type[a]	2.6 ± 0.3	30 ± 1	$(1.2 \pm 0.1) \times 10^7$
D181A[a]	56 ± 2	$(6.5 \pm 0.2) \times 10^{-2}$	$(1.2 \pm 0.1) \times 10^3$
Q262A[b]	0.35 ± 0.05	0.29 ± 0.002	$(8.3 \pm 1.1) \times 10^5$
D181A/Q262A[a]	51 ± 4	$(2.7 \pm 0.1) \times 10^{-3}$	$(5.3 \pm 0.5) \times 10^1$

[a] Measured at 25 °C and pH 7.0. [b] Measured at 30 °C and pH 7.0 (*14*).

Scheme 1

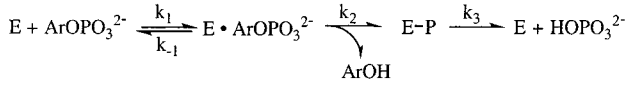

than that of PTP1B while the K_m was 22-fold higher (Table 2). As shown previously, Q262A exhibited 38- and 7.4-fold decrease in K_m for *p*NPP and the $EGFR^{988-998}$ peptide, respectively (*14*). In addition, the k_{cat} for the Q262A-catalyzed hydrolysis of *p*NPP and the $EGFR^{988-998}$ peptide was reduced 80- and 150-fold, respectively (*14*). The substitution of Gln262 by an Ala in D181A resulted in a 33-fold decrease in K_m and an 11-fold decrease in k_{cat} with *p*NPP as a substrate (Table 1). Interestingly, with the $EGFR^{988-998}$ peptide as a substrate, the k_{cat} for D181A/Q262A was 24-fold lower than that of D181A, while its K_m value was similar to that of D181A (Table 2). Collectively, then, it appears that mutation at either Asp181 or Gln262 results in large reductions in k_{cat} irrespective of the substrates, and the k_{cat} for the double mutant is slower than those for the single mutants.

The Kinetic Parameter K_m Is Not an Accurate Indicator of Substrate Binding Affinity. The overall mechanism of the PTPase-catalyzed reaction involves a number of steps that are represented schematically in Scheme 1, where $ArOPO_3^{2-}$ can be either aryl phosphates or pTyr-containing peptides/proteins. The reaction proceeds through a sequence involving substrate binding (substrate dissociation constant $K_s = k_{-1}/k_1$), which is then cleaved with phosphoryl transfer (k_2) to the active site nucleophilic Cys residue (E−P formation). Subsequent general base-catalyzed reaction with water cleaves the phosphoenzyme intermediate E−P (k_3), and release of phosphate completes the catalytic cycle. Applying the steady-state assumption to [E−P], it can be shown that $k_{cat} = [k_2k_3/(k_2 + k_3)]$ and $K_m = [K_sk_3/(k_2 + k_3)]$. Thus, the k_{cat} term describes the rate-limiting step under saturating concentrations of substrate and is mostly determined by the E−P hydrolysis step (k_3) for the wild-type PTP1B (*14*, *40*). The K_m parameter is an apparent dissociation constant that can be treated as the overall dissociation constant of all enzyme-bound species (*41*). For example, when k_2 is much greater than k_3, the concentration of E−P is much greater than $[E{\cdot}ArOPO_3^{2-}]$, so that E−P contributes more to K_m than does $E{\cdot}ArOPO_3^{2-}$ and is the predominant enzyme-bound species. Thus, K_m is not an accurate measure of substrate-binding affinity. Rather, its value is smaller than the substrate dissociation constant K_s by a factor of $k_3/(k_2 + k_3)$.

The dramatic decrease in K_m for the Q262A mutant, which may be indicative of increased accumulation of the E−P intermediate in the Q262A-catalyzed reactions, is consistent with the observations that substitution of Gln262 by an Ala has a more severe effect on k_3 than on k_2 (*12*−*14*). Interestingly, it appears that, for both D181A and the double mutant D181A/Q262A, the mutation may have a more negative effect on k_3 in the *p*NPP reaction, resulting in a decrease in K_m. In contrast, in the peptide substrate reaction, the mutation may have a more deleterious effect on k_2, leading to an increase in K_m. Thus, it is difficult to predict the substrate binding affinity of the double mutant (D181A/Q262A) based purely on the apparent K_m values.

D181A/Q262A Displays Higher Affinity to Ac-Asp-Ala-Asp-Glu-F_2Pmp-Leu-NH_2 than Does D181A. To determine directly the binding affinity for substrates of the PTP1B double mutants, we performed isothermal titration microcalorimetry (ITC) experiments. ITC allows a simultaneous determination of the binding constant (K) and stoichiometry as well as the enthalpy change (ΔH) associated with the binding of a ligand to a macromolecule (*32*). From these parameters, the Gibbs free energy of binding (ΔG) and the entropy change (ΔS) of binding can also be derived from the expression $\Delta G = -RT \ln K = \Delta H - T\Delta S$. Because of the inherent hydrolytic activity, it has not been possible to study directly the binding interactions between a PTPase and its substrate. To compare binding interactions between wild-type PTP1B and its various mutants (either active or inactive), we have used peptides that contain a nonhydrolyzable pTyr analogue, phosphonodifluoromethyl phenylalanine (F_2Pmp), in the ITC experiments (*28*).

The F_2Pmp-containing peptide, Ac-Asp-Ala-Asp-Glu-F_2-Pmp-Leu-NH_2, is an excellent nonhydrolyzable substrate analogue that exhibits high affinity for PTP1B (*28*, *42*, *43*). Using ITC, we have previously determined the dissociation constant (K_d) and thermodynamic parameters for the binding of Ac-Asp-Ala-Asp-Glu-F_2Pmp-Leu-NH_2 to PTP1B and the mutants C215S and D181A (*28*). We showed that the active site Cys215 to Ser mutant PTP1B binds Ac-Asp-Ala-Asp-Glu-F_2Pmp-Leu-NH_2 with the same affinity as the wild-type enzyme (Table 3). In addition, we found that the general acid deficient mutant D181A binds the same ligand 5-fold tighter than the C215S mutant, consistent with the observation that the Asp to Ala mutant is a better substrate-trapping reagent than C215S (*20*, *21*).

To determine whether any one of the double mutants (D181A/Q262A, D181A/C215S, D181A/C215E, and C215S/Q262A) displays improved binding properties over the D181A mutant, we measured the K_d values of the double mutants for Ac-Asp-Ala-Asp-Glu-F_2Pmp-Leu-NH_2 and the thermodynamic parameters associated with binding using ITC under identical conditions (pH 7.0, ionic strength of 0.15 M, and 25 °C) employed for the wild-type PTP1B and the C215S and D181A mutants (Table 3). A typical titration curve and binding isotherm for the binding of D181A/Q262A to Ac-Asp-Ala-Asp-Glu-F_2Pmp-Leu-NH_2 is shown in Figure 3. From curve-fitting of the binding isotherms, the stoichiometry for the binding of the peptide to D181A/Q262A was determined to be 1:1. The dissociation constant K_d was 6.8 nM, which is ~30-fold lower than those of the wild-type PTP1B and the C215S mutant (Table 3). More importantly, D181A/Q262A also exhibits nearly 6-fold higher affinity for Ac-Asp-Ala-Asp-Glu-F_2Pmp-Leu-NH_2 than does the D181A mutant. The association process between D181A/Q262A and

Table 3: Thermodynamic Parameters for the Binding of PTP1B and Its Substrate-Trapping Mutants with Ac-Asp-Ala-Asp-Glu-F_2Pmp-Leu-NH_2[a]

PTP1B	K_d (μM)	ΔH (kcal mol^{-1})	$T\Delta S$ (kcal mol^{-1})	ΔG (kcal mol^{-1})
wild type[b]	0.24 ± 0.05	−3.9 ± 0.2	5.1 ± 0.2	−9.0 ± 0.1
C215S[b]	0.19 ± 0.03	−10.4 ± 0.2	−1.2 ± 0.2	−9.2 ± 0.1
D181A[b]	0.04 ± 0.01	−6.5 ± 0.1	3.7 ± 0.1	−10.2 ± 0.1
D181A/Q262A[c]	0.0068 ± 0.0023	−4.5 ± 0.05	6.6 ± 0.2	−11.1 ± 0.2
D181A/C215E[c]	1.3 ± 0.09	−28.4 ± 0.3	−20.4 ± 0.3	−8.0 ± 0.03

[a] All experiments were performed at 25 °C and pH 7.0. [b] From (*28*). [c] From this study.

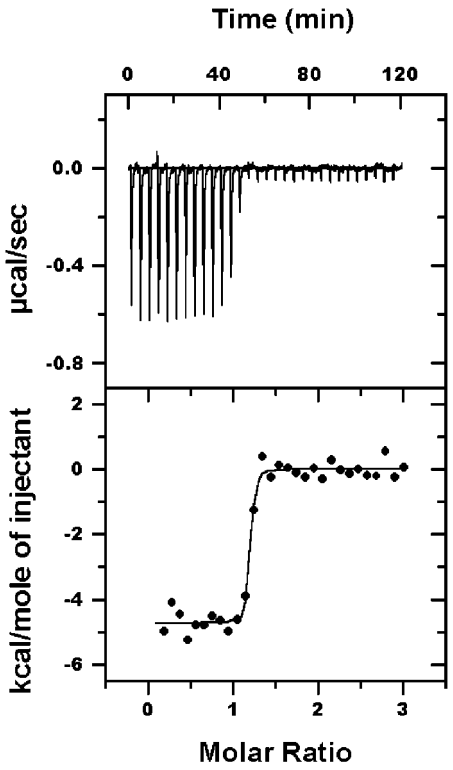

FIGURE 3: Calorimetric isothermal titration for the reaction of peptide Ac-Asp-Ala-Asp-Glu-F_2Pmp-Leu-NH_2 with PTP1B/D181A/Q262A. Top: raw data for 30 8-μL injections of the peptide (0.5 mM stock) into the isothermal cell containing 32 μM PTP1B/D181A/Q262A at 4 min intervals and 25 °C. Both the protein and the peptide were in 50 mM 3,3-dimethylglutarate buffer, $I = 0.15$ M, pH 7.0, containing 1 mM DTT. Bottom: integrated curve showing experimental points that were obtained by integration of the above peaks plotted against the molar ratio of the peptide to PTP1B/D181A/Q262A in the reaction cell. The solid line corresponds to the best fit to the data by a nonlinear least-squares regression algorithm ORIGIN (*32*).

the F_2Pmp-containing peptide is both enthalpically ($\Delta H = -4.5$ kcal/mol) and entropically ($T\Delta S = 6.6$ kcal/mol) favored, yielding a ΔG for binding of −11.1 kcal/mol at pH 7.0 and 25 °C. The increased binding affinity for the D181A/Q262A mutant, as compared to the D181A mutant, appears to result from a larger increase in the $T\Delta S$ term, which more than offset the smaller decrease in ΔH of binding (Table 3).

We were not able to obtain K_d values for D181A/C215S and C215S/Q262A because the titration curves were rather complex. The observed titration curves either yielded a very low binding stoichiometry (~0.1 for D181A/C215S) or displayed two peaks (C215S/Q262A) with one absorbing heat and the other releasing heat (data not shown). We also noted that even for the C215S single mutant, the titration curve also displayed two peaks at a lower temperature (15 °C). Because all of the mutants were purified to homogeneity (i.e., a single band in SDS−PAGE), these observations suggest that the C215S-containing mutants may exist in aqueous solution as an equilibrium mixture of more than one conformation. Indeed, the recently solved crystal structure of the apo PTP1B/C215S mutant showed that C215S can exist in a conformation that is different from that observed in the C215S/substrate complex (*44*). It is possible that removal of the negative charge from the thiolate group in Cys215 may lead to a disruption of the active site conformation (*28*). However, we were able to obtain the K_d and thermodynamic parameters for the binding of Ac-Asp-Ala-Asp-Glu-F_2Pmp-Leu-NH_2 to D181A/C215E (Table 3). The affinity of D181A/C215E for the peptide ($K_d = 1.3$ μM) is 7- and 32-fold fold lower than those of the C215S and D181A mutants, respectively. Thus, substitution of Cys215 in PTP1B/D181A does not improve PTP1B's affinity for substrates. By contrast, substitution of Gln262 by an Ala in PTP1B/D181A generates a much improved PTP1B substrate-trapping mutant, with a binding affinity 6-fold higher than that of PTP1B/D181A.

D181A/Q262A Is a Better Substrate-Trapping Mutant than D181A in Vivo. From the experiments described above, we have shown that the D181A/Q262A mutant not only displays lower catalytic activity than the D181A mutant, but also exhibits higher binding affinity toward a peptide substrate analogue. In the following, we present evidence that D181A/Q262A is also a better substrate-trapping mutant in vivo.

To determine whether the double mutant D181A/Q262A also possesses higher affinity for physiological substrates of PTP1B, we performed substrate-trapping experiments in COS1 cells. It has been shown previously that, in COS1 cells, the EGF receptor is the major substrate for PTP1B, and that the D181A mutant has a higher affinity for the EGF receptor than does the C215S mutant (*21*). Because EGF receptor is the major PTP1B substrate in COS1 cells, we wanted to determine the effects of expression of PTP1B and its various forms of trapping mutants, in this cell type, on the level of EGF receptor tyrosine phosphorylation. We therefore expressed the full-length HA-tagged wild-type, D181A, C215S, D181A/Q262A, and D181A/C215S mutants of PTP1B in COS1 cells, and then immunoblotted the cell lysates with an anti-pTyr antibody (Figure 4). The protein expression level of wild-type and mutant PTP1Bs was shown to be similar by Western blotting of the cell lysates using anti-HA antibodies (Figure 4). Consistent with the earlier work (*21*), we found that the level of pTyr in EGF receptor in cells expressing wild-type PTP1B was comparable to that in the vector control. In addition, we also noted that the tyrosine phosphorylation level of EGF receptor was higher in cells expressing the D181A mutant than C215S (Figure 4). These results serve as important controls to demonstrate that, as

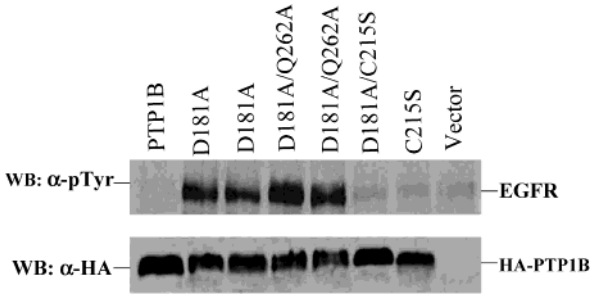

FIGURE 4: Level of tyrosine phosphorylation in the EGF receptor upon expression of the wild-type and mutant PTP1Bs (4 μg of plasmid/60 mm dish) in COS1 cells. Samples (50 μg of protein) from the COS1 cell lysates were separated by SDS−PAGE and transferred onto a nitrocellulose membrane. The proteins on the membrane were first immunoblotted with anti-pTyr HRP conjugate (upper panel). The membrane was then stripped and reprobed with anti-HA HRP conjugate (lower panel).

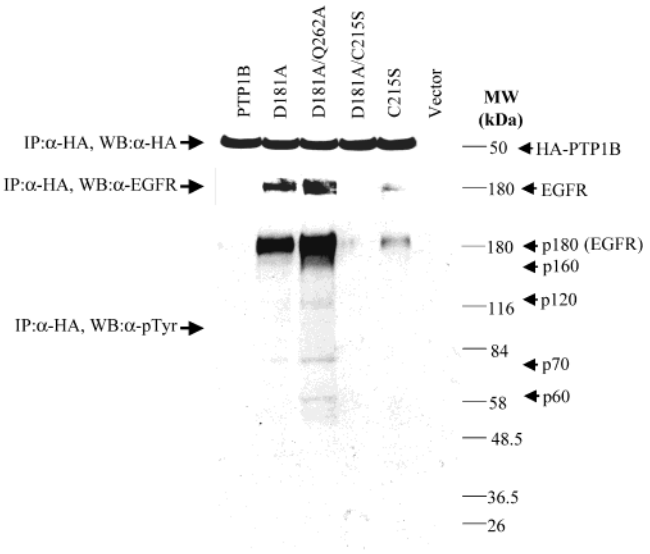

FIGURE 5: Immunoprecipitation of PTP1B substrates by the PTP1B substrate-trapping mutants. Wild-type PTP1B, D181A, D181A/Q262A, D181A/C215S, C215S, and blank vector (pJ3H) were used to transfect COS1 cells (4 μg of plasmid/60 mm dish). The cells were maintained at 37 °C for 44−48 h. Twenty minutes before harvesting the cells, 20 ng/mL EGF was added to each dish. The PTP1B proteins were precipitated using anti-HA antibody conjugated agarose beads from the cell lysates (500 μg of total protein) at 4 °C overnight. The beads were washed 3 times with the lysis buffer, mixed with 2× SDS sample buffer, and then boiled for 5 min. The immuno-complexes were resolved by SDS−PAGE, and transferred onto a nitrocellulose membrane. The membrane was probed with anti-pTyr HRP-conjugated antibody (lower panel). The membrane was then stripped and reblotted with the anti-HA HRP conjugate to visualize the HA-tagged PTP1B (upper panel). Thereafter, the membrane was further stripped, and reprobed with anti-EGFR rabbit polyclonal antibody (middle panel).

shown previously, D181A has higher affinity for EGF receptor than does C215S, and that the trapping mutants bind to and protect substrates from dephosphorylation by endogenous PTPases.

We next evaluated the ability of D181A/Q262A and D181A/C215S to promote accumulation of the pTyr-phosphorylated EGF receptors in COS1 cells. We discovered that D181A/C215S displayed a comparable affinity to that of C215S (Figure 4). By contrast, we were satisfied to find that enhancement of EGF receptor phosphorylation was most pronounced in cells expressing D181A/Q262A than any other PTP1B mutants (Figure 4). Immunoblotting of the cell lysates with anti-pTyr antibodies showed that the D181A/Q262A mutant was more than 3-fold better than the D181A mutant in protecting the phosphorylated EGF receptors in COS1 cells. These data suggest that D181A/Q262A displays the highest binding affinity among all mutant forms of PTP1B applied in our experiments and it can strongly protect the EGF receptor from dephosphorylation by endogenous PTPases.

Finally, we determined whether the binding interaction between the trapping mutants and the substrate would be stable enough to endure isolation procedures. We expressed the wild-type and the mutant forms of PTP1B in COS1 cells. After the cells were treated with EGF (20 ng/mL for 20 min), the expressed PTP1B proteins were immunoprecipitated from the cell lysates using anti-HA antibody conjugated agarose. The associated substrates were visualized by anti-pTyr and anti-EGFR immunoblotting, and the amount of co-immunoprecipitated PTP1B was measured with HRP-conjugated anti-HA antibody. As shown in Figure 5, the wild-type and mutant PTP1Bs were expressed to similar levels. D181A/C215S displayed a weaker affinity than C215S. More importantly, the D181A/Q262A mutant coprecipitated more than 3-fold greater quantities of tyrosine-phosphorylated EGF receptor than did the D181A mutant. In addition, the amount of EGF receptor protein associated with D181A/Q262A and D181A also corresponded to the level of pTyr in the EGF receptor, suggesting that only the phosphorylated EGF receptor bound to the trapping mutants (Figure 5). Moreover, the D181A/Q262A double mutant also trapped several novel, less abundant tyrosine-phosphorylated proteins (e.g., p160, p120, p70, and p60 in Figure 5) that were not visible in either the D181A or the C215S sample. This is rather impressive, since EGF receptor is very abundant in COS1 cells (*21*). Pre-clearance of the EGF receptor from the cell lysates with anti-EGFR antibodies before substrate trapping would enhance the binding of less abundant substrates with D181A/Q262A. Work is in progress to identify these novel PTP1B substrates. Collectively, we have demonstrated from both substrate protection and substrate pull-down experiments that D181A/Q262A is a substrate-trapping mutant superior to D181A.

Summary. Based on insights from mechanistic studies, we designed several mutant PTP1Bs in order to create substrate-trapping mutants with improved properties over the existing mutants. Kinetic and thermodynamic characterization indicated that PTP1B/D181A/Q262A possesses further decreased catalytic activity and increased substrate-binding affinity than does PTP1B/D181A. These properties suggest that D181A/Q262A would serve as an improved substrate-trapping mutant, as compared with D181A. Indeed, in vivo substrate trapping experiments indicated that this is the case: D181A/Q262A displayed higher affinity than D181A for a bona fide PTP1B substrate, the EGF receptor. Further, D181A/Q262A can also trap several novel, less abundant protein substrates that were missed by D181A. Thus, this newly developed and improved substrate-trapping mutant can be used as a powerful affinity reagent to isolate and purify PTP1B physiological substrates. Because of the conserved roles of Asp181 and Gln262 in PTPase catalysis and the proximity of these residues to the active site (pTyr pocket), it is unlikely that

D181A/Q262A and D181A would exhibit substrate specificity different from that of the wild-type enzyme. Furthermore, given that both Asp181 and Gln262 are invariant among the PTPase family, it is predicted that this improved substrate-trapping mutant would be applicable to all members of PTPase family for the identification of physiological substrates.

REFERENCES

1. Neel, B. G., and Tonks, N. K. (1997) *Curr. Opin. Cell Biol. 9*, 193−204.
2. Li, L., and Dixon, J. E. (2000) *Semin. Immunol. 12*, 75−84.
3. Zhang, Z.-Y. (2001) *Curr. Opin. Chem. Biol. 5*, 416−423.
4. International Human Genome Sequencing Consortium. (2001) *Nature 409*, 860−921.
5. Zhang, Z.-Y. (1998) *Crit. Rev. Biochem. Mol. Biol. 33*, 1−52.
6. Guan, K. L., and Dixon, J. E. (1991) *J. Biol. Chem. 266*, 17026−17030.
7. Cho, H., Krishnaraj, R., Kitas, E., Bannwarth, W., Walsh, C. T., and Anderson, K. S. (1992) *J. Am. Chem. Soc. 114*, 7296−7298.
8. Zhang, Z.-Y., Wang, Y., and Dixon, J. E. (1994) *Proc. Natl. Acad. Sci. U.S.A. 91*, 1624−1627.
9. Hengge, A. C., Sowa, G., Wu, L., and Zhang, Z.-Y. (1995) *Biochemistry 34*, 13982−13987.
10. Wu, L., and Zhang, Z.-Y. (1996) *Biochemistry 35*, 5426−5434.
11. Denu, J. M., Lohse, D. L., Vijayalakshmi, J., Saper, M. A., and Dixon, J. E. (1996) *Proc. Natl. Acad. Sci. U.S.A. 93*, 2493−2498.
12. Zhao, Y., Wu, L., Noh, S. J., Guan, K.-L., and Zhang, Z.-Y. (1998) *J. Biol. Chem. 273*, 5484−5492.
13. Pannifer, A. D. B., Flint, A. J., Tonks, N. K., and Barford, D. (1998) *J. Biol. Chem. 273*, 10454−10462.
14. Sarmiento, M., Zhao, Y., Gordon, S. J., and Zhang, Z.-Y. (1998) *J. Biol. Chem. 273*, 26368−26374.
15. Zhang, Y.-L., Hollfelder, F., Gordon, S. J., Chen, L., Keng, Y.-F., Wu, L., Herschlag, D., and Zhang, Z.-Y. (1999) *Biochemistry 38*, 12111−12123.
16. Hoff, R. H., Wu, L., Zhou, B., Zhang, Z.-Y., and Hengge, A. C. (1999) *J. Am. Chem. Soc. 121*, 9514−9521.
17. Bliska, J. B., Clemens, J. C., Dixon, J. E., and Falkow, S. (1992) *J. Exp. Med. 176*, 1625−1630.
18. Sun, H., Charles, C. H., Lau, L. F., and Tonks, N. K. (1993) *Cell 75*, 487−493.
19. Milarski, K. L., Zhu, G., Pearl, C. G., McNamara, D. J., Dobrusin, E. M., Maclean, D., Thieme-Sefler, A., Zhang, Z.-Y., Sawyer, T., Decker, S. J., Dixon, J. E., and Saltiel, A. R. (1993) *J. Biol. Chem. 268*, 23634−23639.
20. Garton, A. J., Flint, A. J., and Tonks, N. K. (1996) *Mol. Cell. Biol. 16*, 6408−6418.
21. Flint, A. J., Tiganis, T., Barford, D., and Tonks, N. K. (1997) *Proc. Natl. Acad. Sci. U.S.A. 94*, 1680−1685.
22. Liu, F., Hill, D. E., and Chernoff, J. (1996) *J. Biol. Chem. 271*, 31290−31295.
23. Black, D. S., and Bliska, J. B. (1997) *EMBO J. 16*, 2730−2744.
24. Buist, A., Blanchetot, C., Tertoolen, L. G., and den Hertog, J. (2000) *J. Biol. Chem. 275*, 20754−20761.
25. Weng, L.-P., Wang, X., and Yu, Q. (1999) *Genes Cells 4*, 185−196.
26. Noguchi, T., Tsuda, M., Takeda, H., Takada, T., Inagaki, K., Yamao, T., Fukunaga, K., Matozaki, T., and Kasuga, M. (2001) *J. Biol. Chem. 276*, 15216−15224.
27. Andersen, J. N., Mortensen, O. H., Peters, G. H., Drake, P. G., Iversen, L. F., Olsen, O. H., Jansen, P. G., Andersen, H. S., Tonks, N. K., and Moller, N. P. (2001) *Mol. Cell. Biol. 21*, 7117−7136.
28. Zhang, Y.-L., Yao, Z.-J., Sarmiento, M., Wu, L., Burke, T. R., Jr., and Zhang, Z.-Y. (2000) *J. Biol. Chem. 275*, 34205−34212.
29. Puius, Y. A., Zhao, Y., Sullivan, M., Lawrence, D. S., Almo, S. C., and Zhang, Z.-Y. (1997) *Proc. Natl. Acad. Sci. U.S.A. 94*, 13420−13425.
30. Zhang, Y.-L., and Zhang, Z.-Y. (1998) *Anal. Biochem. 261*, 139−148.
31. Zhang, Z.-Y., Thieme-Sefler, A. M., Maclean, D., Roeske, R., and Dixon, J. E. (1993) *Anal. Biochem. 211*, 7−15.
32. Wiseman, T., Williston, S., Brandts, J., and Lin, L.-N. (1989) *Anal. Biochem. 179*, 131−137.
33. Sells, M. A., and Chernoff, J. (1995) *Gene 152*, 187−189.
34. Laemmli, U. K. (1970) *Nature 227*, 680−685.
35. Zhang, Z.-Y., and Wu, L. (1997) *Biochemistry 36*, 1362−1369.
36. Zhang, Z.-Y., and Dixon, J. E. (1993) *Biochemistry 32*, 9340−9345.
37. Juszczak, L. J., Zhang, Z.-Y., Wu, L., Gottfried, D. S., and Eads, D. D. (1997) *Biochemistry 36*, 2227−2236.
38. Wang, F., Li, W., Emmett, M. R., Hendrickson, C. L., Marshall, A. G., Zhang, Y.-L., Wu, L., and Zhang, Z.-Y. (1998) *Biochemistry 37*, 15289−15299.
39. Jia, Z., Barford, D., Flint, A. J., and Tonks, N. K. (1995) *Science 268*, 1754−1758.
40. Zhang, Z.-Y. (1995) *J. Biol. Chem. 270*, 11199−11204.
41. Fersht, A. (1985) *Enzyme Structure and Mechanism*, 2nd ed., pp 104−105, W. H. Freeman & Co., New York.
42. Burke, T. R., Jr., Smyth, M., Nomizu, M., Otaka, A., and Roller, P. P. (1993) *J. Org. Chem. 58*, 1336−1340.
43. Chen, L., Wu, L., Otaka, A., Smyth, M. S., Roller, P. P., Burke, T. R., den Hertog, J., and Zhang, Z.-Y. (1995) *Biochem. Biophys. Res. Commun. 216*, 976−984.
44. Scapin, G., Patel, S., Patel, V., Kennedy, B., and Asante-Appiah, E. (2001) *Protein Sci. 10*, 1596−1605.

BI015904R